

Theoretical Analysis and Experiment of Liquid Metal Penetration into Slot Plug Applied for Refining Ladles

ZHONGFU CHENG and MIAOYONG ZHU

Penetration phenomena of liquid metal into a slot plug is applicable to a wide range of refining ladles. In the current work, slot plug parameters, especially the slot width, which is the most important factor for operational safety, were studied by analyzing the penetration mechanism in using interfacial theory. A theoretical model for predicting the relationship of plug parameters and liquid metal bath depth is proposed. Furthermore, a simple approach of measuring penetration depth and flow behavior of liquid metal is presented. The corresponding experiment validating the model was successfully performed with Wood's metal. The results show that factors affecting the penetration of liquid metal into slot plug include slot geometric parameters, surface roughness, and ambient pressures. Of these, slot width is the primary factor determining the penetration, and the effect of slot length can be ignored when it reaches 50 times the width. The penetration process of liquid metal into slot plug can be divided into three stages: unsteady penetration, main penetration, and terminal penetration. Increasing the uniformity of slot width along the length direction can extend the service life of slot plug.

DOI: 10.1007/s11663-014-0093-0

© The Minerals, Metals & Materials Society and ASM International 2014

I. INTRODUCTION

POROUS plugs and slot plugs made of refractory bricks are widely used to blow gases into liquid metal in refining ladles. During the blowing interval, liquid metal will penetrate into the plugs due to the static pressure of liquid metal and consequently will block and damage the plugs, resulting in the deterioration of ladle refining. Therefore, penetration phenomenon of liquid metal into refractory bricks is of a great importance in metallurgical processes and attracts great interest from metallurgical researchers and workers.

Recently, Zhu and his coworkers^[1-3] developed a new technology of bottom powder injection for ladle refining as shown in Figure 1. This technology not only has the function of argon blowing, but also has the function of powder injection with the original technical layout. Compared with the traditional injection method with submerged lance,^[4-7] the new technology has many advantages, such as better thermodynamic and kinetic conditions, less serious splashing, higher powder utilization, and higher desulphurization rate. In addition, there is also no steel cleanliness risk caused by lance refractory. The key of this new technology is to design a powder injection device, which is able to inject powders smoothly with penetration resistance. Among various injection plugs, slot plug is well known for its ability of preventing penetration, and recently it has been successfully applied for powder injection.^[1-3] Thus, the slot plug is an optimum choice for

this new technology, and the penetration phenomenon of liquid metal into this plug has to be deeply understood to determine the design parameters. A predictive equation is required to a variety of plug types, and a measuring technique is in demand to provide both qualitative and quantitative penetration information.

Previous studies related to the penetration of liquid metal into refractory plugs have involved both physical and mathematical modeling. Early works on the penetration of liquid metal into porous refractory were performed by analyzing the cooling specimens or established water model.^[8,9] With the development of high-temperature X-ray radiography, it is possible to observe the penetration process of liquid metal into refractory directly,^[10] and a series of significant work was carried out subsequently. Li *et al.*^[11] investigated the penetration behavior of molten silver into porous refractory by analyzing the image records, and they found that there was a critical external pressure over which the penetration depth increased with external pressure. They employed the penetration models of liquids into a vertical capillary to illustrate this penetration phenomenon.^[12] Matsushita *et al.*^[13] analyzed the evaluation of labyrinth factor for porous plug, and in their later research, they pointed out that the value of labyrinth depended on the refractory material, the porous distribution, and the properties of liquid metal.^[14] From 2001 to 2004, a series of penetration experiments^[14-17] was carried out to understand the penetration behavior of liquid metals into porous refractory, and the penetration process was divided into two stages: prepenetration stage and bulk-penetration stage. For this two-stage mechanism, different modifications of classic capillary were proposed.^[18] At the same time, the variation of penetration rate was presented after a series of studies,^[19-22] and it was found that the penetration

ZHONGFU CHENG, Ph.D. Candidate, and MIAOYONG ZHU, Professor, are with the School of Materials and Metallurgy, Northeastern University, Shenyang 110819, Liaoning, P.R. China. Contact e-mail: myzhu@mail.neu.edu.cn

Manuscript submitted July 9, 2013.

Article published online July 2, 2014.

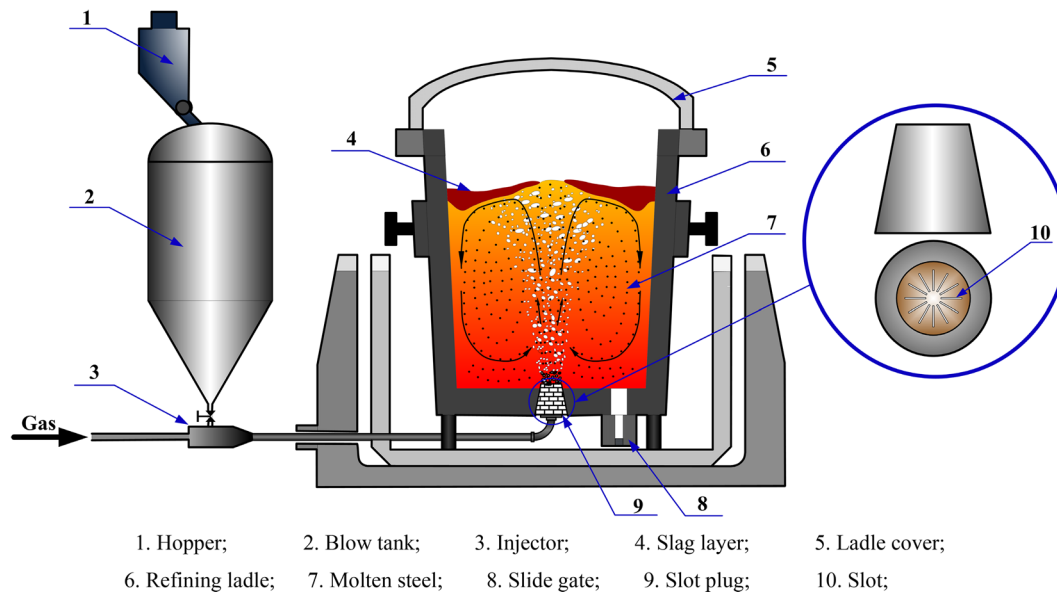


Fig. 1—Schematic diagram of bottom powder injection in a new refining ladle.

depth was almost proportional to the square root of time at the initial stage,^[18,21,22] then it remained nearly a constant value. Mukai *et al.*^[22] attributed the stop of penetration to the increased viscosity and surface tension of liquid metal, and the reduced pore size of refractory. All the above-mentioned research is very helpful to understand the penetration mechanism of liquid metals into porous refractory plugs.

However, to the penetration phenomenon of liquid metal into slot plug, the various parameters associated with them have not been sufficiently understood. It has its own penetration characteristics requiring further study, and there remains an interest in developing a better understanding of penetration behavior. Previous researchers^[1,23] devised the slot width mainly depending on Barthel's model,^[24] in which the rectangular slot was treated as a circular hole. But for the slot plug, the geometric parameters (e.g., slot width and length), surface roughness, *etc.*, have an important influence on the penetration process. This is consistent with the experimental results of molten steel penetrating into directional type plug.^[25] Up to now, the mechanism of liquid metal penetration into a slot plug has been rarely reported.

In this article, a penetration model was established to accurately describe the relationship between slot geometric parameters (especially the safe slot width) and liquid metal bath depth, and a simple approach to monitor electrical signal was proposed to measure penetration depth and flow behavior. The corresponding experiment with Wood's metal was carried out to validate the current penetration theory.

II. THEORETICAL ANALYSIS

Slot plugs are usually installed at the bottom of a refining ladle, through which gases or powders can be

injected into the liquid metal bath. During the blowing interval, a slot plug without penetration of liquid metal becomes the prerequisite for bottom injection. The major concern is to protect slot plug from the penetration of liquid metal. The penetration is usually influenced by many factors, such as slot geometric parameters (slot width and length), surface roughness, ambient pressures, *etc.*, among which slot width is the primary one. For a certain bath depth, there is a critical slot width. If the real slot width exceeds that value, then liquid metal will penetrate into the plug. This value is defined as a key parameter here, namely safe slot width, and it is commonly used in the following sections. The goal of this section is to build a theoretical model to predict the safe slot width with a function of liquid metal bath depth.

A. Safe Slot Width

Because liquid metal above slot plug contacts with refractory surface, there exists an adhesive force between liquid metal and refractory. The adhesive force can prevent liquid metal from slipping along the refractory wall downward. There is also a cohesive force in liquid metal, which can prevent the surface of liquid metal from tearing. Hence, the liquid metal in slot can form a liquid film on the gas–liquid interface to withstand a certain amount of static pressure. Both of the two forces have their limits. If the cohesive force reaches its limit earlier than the adhesive one, then liquid metal will penetrate into the slot by tearing the film. Liquid metal cannot penetrate into the slot according to this mechanism in actual situation, as there is no liquid film torn on the gas–liquid interface. Therefore, adhesive force is the key to determine whether liquid metal penetrates into slot. In the current work, it is assumed that there is no chemical interaction between liquid metal and slot plug, and the liquid metal is inert. Details of penetration process controlled by this mechanism are revealed as follows.

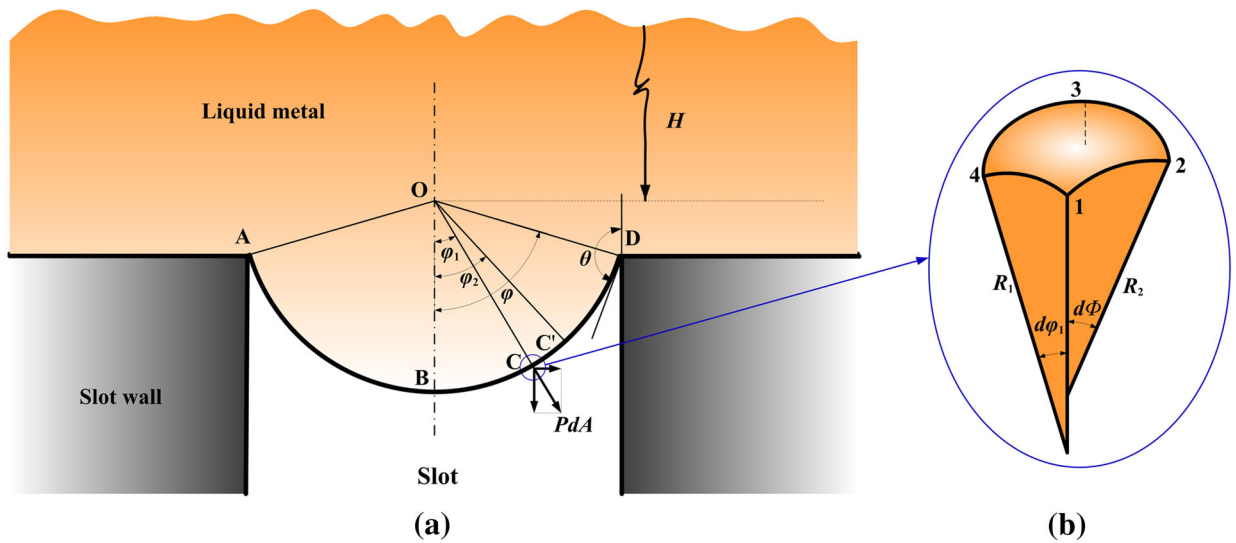


Fig. 2—Schematic illustration of (a) forces acting on the liquid film and (b) microcell and surface area.

As Figure 2 illustrates, liquid metal with density ρ is in a liquid metal bath with depth H . A slot plug is installed at the bottom of the bath. The width of the slot is δ and the length is W . The AD arc line stands for a liquid film with the radius R , and the force analysis of the random point C on AD film is illustrated in Figure 2(a), where φ_1 is the angle between OB and OC. The contact angle between liquid metal and refractory is θ , where, $\theta = \varphi + \pi/2$, and $R = \delta/(2\cos\theta)$.

When the adhesive force reaches its limit, the whole liquid film will move down along the slot wall, which will produce a relative slipping. But the real situation is that liquid metal is a continuum fluid. As it penetrates into a slot, it will spread on the wall and form a new contact surface. To prevent penetration, the forces acting on the liquid film have to be balanced; namely, the additional pressure P_{add} should balance with the static pressure P_{sta} , where P_{add} is produced by the bend of gas–liquid interface, and P_{sta} equals ρgH .

When liquid metal penetrates into the slot, the gas–liquid interfacial film will bend along the width and length directions. Figure 2(b) is the microcell of liquid film corresponding to microarc CC' in Figure 2(a), where, R_1 is the radius of curvature at the curves of 14 and 23 in the length direction, and R_2 is the radius of curvature at the curves of 12 and 34 in the width direction. The additional pressure P_{add} can be calculated from the Young-Laplace equation, namely

$$P_{\text{add}} = \sigma \left(\frac{1}{R_1} + \frac{1}{R_2} \right) \quad [1]$$

where σ is the surface tension of liquid metal. Considering the slot geometric shape, additional pressure P_{add} is given as

$$P_{\text{add}} = -\frac{2\sigma \cos\theta}{\delta} \left(1 + \frac{\delta}{W} \right) \quad [2]$$

The cross-sectional surface of the slot is a rectangle, and the geometric feature is contained in the term of δ/W .

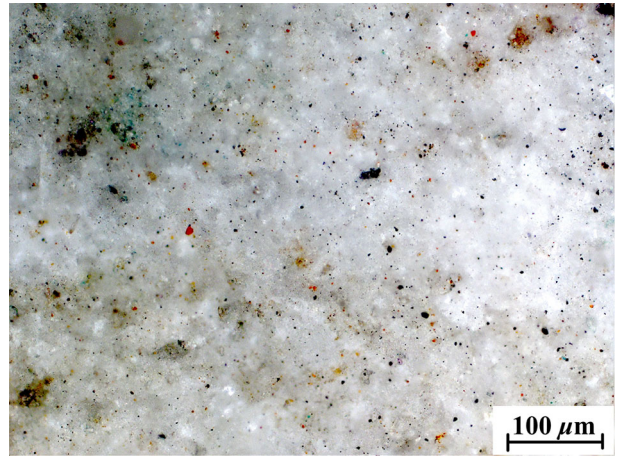


Fig. 3—The surface morphology of corundum refractory.

The slot plug is vertically assembled at the bottom of a refining ladle. In some cases, the pressure in the ladle does not balance with that in the slot plug. It is comprehensive to take ambient pressures into consideration. Here, the ambient pressures include the environmental pressure P_0 in liquid metal bath and the residual pressure P in the slot plug. To prevent penetration, the sum of the additional pressure P_{add} and the residual pressure P has to be equal to that of the static pressure P_{sta} and the environmental pressure P_0 .

As these two ambient pressures have been taken into account, the equilibrium equation will be written as

$$P_0 + P_{\text{sta}} = P_{\text{add}} + P \quad [3]$$

Finally, the expression for calculating the safe slot width can be given as

$$\delta = -\frac{2\sigma \cos \theta}{P_0 + \rho g H - P} \cdot \left(1 + \frac{\delta}{W}\right) \quad [4]$$

where Eq. [4] considers the influences of ambient pressures (P_0 and P) and the slot shape. The above analysis treats the refractory surface as ideally smooth; in other words, the effect of surface roughness on the wetting process was not considered. Obviously, this deviates from the surface character of refractory material. Equation [4] has to be modified to permit the design of plug parameters. In the next section, the influence of surface roughness is taken into account.

B. Roughness Influence

Surface roughness mainly affects the wetting angle between the liquid metal and the refractory. According to various wetting angles, Spori *et al.*^[26] classified surface wettings into five types, namely, ideally smooth surface wetting (Young-type wetting), Wenzel-type wetting, Cassie-type wetting, pinning (a growing drop pained by one obstacle), and Hemiwicking. There may be one or several types of wetting on a rough surface, and some types of wetting can convert into others on certain conditions. For example, the Cassie-type wetting can turn into Wenzel type wetting irreversibly with the action of gravity or outside interference (static pressure, interface contaminate, *etc.*)^[27–29]

Figure 3 shows a typical surface of the refractory material. Usually, the refractory surface is covered with tiny pores, and the types of wetting may be one, two, or even three of the abovementioned types, such as Wenzel-type, Cassie-type or both Wenzel and Cassie types. To give a general expression of the roughness influence on safe slot width, different wetting types have been fully considered as discussed next.

For the Wenzel-type wetting, the roughness influence on the contact angle θ is described by employing a roughness factor^[26] r , namely

$$\cos \theta^W = r \cdot \cos \theta \quad [5]$$

where θ^W is the contact angle considering the Wenzel-type wetting. For the Cassie-type case, Eq. [5] was modified by introducing the fractions r_1 and r_2 , where r_1 corresponds to the area in contact with the liquid divided by the projected area and r_2 stands for the area in contact with the air trapped beneath the drop, also divided by the projected area,^[26] namely

$$\cos \theta^C = r_1 \cdot \cos \theta - r_2 \quad [6]$$

where θ^C is the contact angle considering the Cassie-type wetting. Compared with Eqs. [5] and [6] has a similar form except for the additional term r_2 on the right side, which inspires an attempt to combine these two equations. Two correction coefficients are introduced to consider the influence of surface roughness, including the Wenzel-type wetting and Cassie-type wetting, and a more general equation describing the wetting angle is given as

$$\cos \theta' = k \cdot \cos \theta - d \quad [7]$$

For this equation, θ' is the practical contact angle of liquid metal on a rough surface, and both k and d are correction coefficients, which strongly depend on the wetting behavior. For example, if the Wenzel-type wetting plays a major role, then k equals approximately to the value of r and $d \approx 0$, while the Cassie-type wetting is the leading role, k and d equal approximately to r_1 and r_2 , respectively. Naturally, if both Wenzel-type and Cassie-type wetting work together, then k contains the components of r and r_1 from different wetting types, and d mainly refers to the area ratio of contacting with the trapped air beneath the drop. It is recommended the values of the two correction coefficients are measured experimentally.

Equation [7] is substituted into Eq. [4] to consider the surface roughness influence of refractory material, and the modified equation of calculating safe slot width can be given as

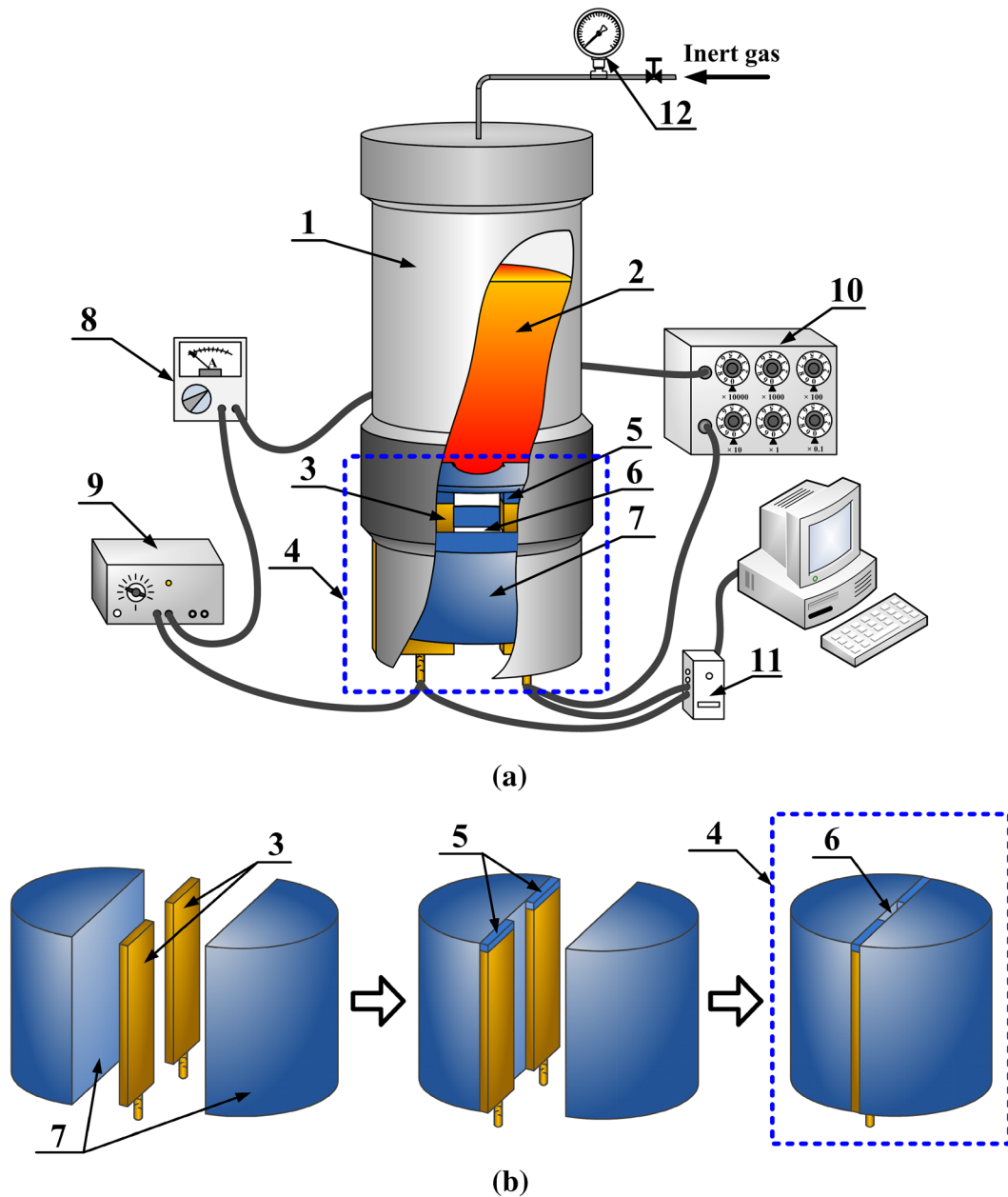
$$\delta = -\frac{2\sigma(k \cos \theta - d)}{P_0 + \rho g H - P} \cdot \left(1 + \frac{\delta}{W}\right) \quad [8]$$

The influence of slot geometric parameters, surface roughness, and ambient pressures are all contained in Eq. [8]. A safe slot width obtained from Eq. [8] is about 1.5 to 3.0 times than that of Eq. [4].

III. SUMMARY OF EXPERIMENTAL APPROACH AND CONDITIONS

To verify the predication theory of safe slot width, a relevant experiment should be carried out because it is difficult to dynamically monitor the penetration behavior. Since the high-temperature X-ray technology has been widely used to observe directly the penetration depth in previous work, it might be a good choice to dynamically detect the penetration process. Unfortunately, this technique is confined for further application because of some limitations, such as high cost, strong radiation, poor safety, *etc.* Hence, in the current work, a new approach for monitoring penetration behavior has been explored and tried. Unlike the previous method, the new approach introduced a circuit to measure the penetration depth by monitoring the electronic signal. The related experimental apparatus was developed successively, and a detail of each part of the apparatus is described as follows.

Figure 4(a) shows the schematic of the experimental apparatus, which mainly consists of a slot plug, an external pressure control system, a liquid metal bath, and a measuring circuit. In the plug, only one slot is designed, which can provide a great convenience for dynamically monitoring penetration process. The slot plug is made up of a pair of semicylindrical refractory bricks, a pair of sheet electrodes with predetermined thickness, and a slot. To clearly illustrate the specific



1. Liquid metal bath; 2. Liquid metal; 3. Sheet electrodes with a predetermined thickness; 4. Slot plug;
 5. Gap filled with refractory; 6. Slot; 7. Semi-cylindrical refractory brick; 8. Ammeter;
 9. Regulated direct powder supply; 10. Protective resistance; 11. Data processor; 12. Pressure gauge;

Fig. 4—Schematic illustration of (a) experimental apparatus for measuring the penetration process of liquid metal into slot plug and (b) the installation process of the slot plug.

structure of the slot plug, a line sketch of its installation process is shown in Figure 4(b). It can be observed from this figure that the slot is surrounded with a pair of semicylindrical refractory bricks and a pair of sheet electrodes. Moreover, the slot width equals the electrode thickness, and the slot length equals the parallel distance between the two electrodes. The fixed slot plug is installed at the bottom of a liquid metal bath, and its ends are inserted into the measuring circuit through the two electrodes. Yet if the electrode tops contact with liquid metal, then the measuring circuit will be directly

conducted. To avoid this situation, a gap between the electrode tops and liquid metal bath has to be reserved. Here, the reserved gap is filled with refractory material, and its depth is 3 mm.

Liquid metal bath is on the top of the slot plug. It is a tough and complex work to change its depth by pouring liquid metal without a larger fluctuation. Thus, an approach has been employed to translate external pressure into static pressure. To start with this, a certain amount of liquid metal is first added in the bath, and then inert gas is injected through a pressure-control

system. By controlling the external pressure of bath room, the equivalent depth of the liquid metal bath can be adjusted continuously. Specifically, as long as the pressure is kept at a required value, the equivalent depth can be calculated. The relationship of equivalent depth of liquid metal bath H and external pressure P_{ext} can be written as

$$H = H' + \frac{P_{\text{ext}}}{\rho g} \quad [9]$$

where H' is the actual depth of liquid metal bath, P_{ext} is the external pressure in the bath room, and H is the equivalent depth of liquid metal bath, which is employed generally in the following sections.

The measuring circuit consists of a direct current (DC) power supply, an ammeter, a protective resistance, and a data processor. The resistance value between the electrodes is very large before liquid metal penetrates into the slot. While penetration takes place, the resistance value will decrease and give rise to a change of electrical signal. The decrease of resistance value between the two sheet electrodes depends on the increase of penetration depth. The quantitative measurement of penetration depth is obtained by collecting the changing electrical signals. The relationship between penetration depth h and electrical signal is given as

$$h = \frac{\rho_{\text{elec}} W}{\delta} \cdot \frac{I}{U} \quad [10]$$

where ρ_{elec} , the conductivity of liquid metal, is for Wood's metal;^[30] I is the current in measuring circuit; and U is the voltage between the two sheet electrodes.

Wood's metal consists of Bi, Pb, Sn, and Cd and is well known for its low melting point. It was selected for the penetration experiment to avoid high-temperature operation, and its physical properties are shown in Table I. The melting point of the selected metal here is about 343 K (70 °C) and can be easily reached in the laboratory. Because the semicylindrical bricks (corundum mainly) contact with the liquid metal directly, at the beginning of the validation experiment, the contact angle between Wood's metal and the corundum bricks was measured with the value of 116.9 deg. The penetration test with Wood's metal was performed in an Ar atmosphere.

The experimental apparatus was used to study the effect factors on liquid metal penetration into a slot plug and to verify the predicted safe slot width as well. Moreover, the variation of penetration depth can be monitored dynamically in the penetration process. The verification experiment was carried out in a thermostat at 378 K (105 °C), and the slot length/width to verify the safe slot width/length were set as 15 mm and 0.08 mm, respectively. Two sets of experiments, denoted as Group A and Group B, have been performed to measure the

dynamical variation of the penetration depth. The relevant parameters and experimental conditions are listed in Table II.

IV. RESULTS AND DISCUSSION

A. Factors Affecting Liquid Metal Penetration into Slot Plug

The relationship between safe slot width and Wood's metal bath depth is shown in Figure 5, and the classic cylindrical capillary model,^[1,18,24] present prediction, and measured profiles are compared in this figure. Overall, the experimental results are lower than the prediction of the cylindrical capillary model and are higher than those calculated by Eq. [4]. That is because the slot feature size, mainly the width and length, was not fully considered in the cylindrical capillary model. If the radius of a cylindrical capillary is equal to the slot width, then the cylindrical capillary will have a stronger capability to resist penetration. In Eq. [4], although the slot feature size with a new term of δ/W has been considered, it does not involve the actual refractory surface conditions, *e.g.*, roughness, heterogeneousness, *etc.*, which leads to the lower prediction unsurprisingly. Therefore, neither the classic cylindrical capillary model nor the ideal surface slot model can exactly predict the relationship between safe slot width and liquid metal bath depth. Equation [8] therefore may be a better choice.

The experimental results also indicate that slot surface roughness enhances the prevention capability from penetration. That is also in accordance with the Tatsu-uya's conclusion.^[25] Thus, it is more reasonable to calculate the safe slot width with Eq. [8]. But this equation cannot be applied directly due to the two unknown coefficients k and d . To obtain the values of k and d , a curve was fitted from the experimental results as shown in the figure. The refractory surface is relatively smooth and d equals approximately 0.1. Based on the fitting curve, the value of k can be obtained, namely 1.4, so Eq. [8] can be rewritten as

$$\delta = -\frac{2\sigma(1.4 \cos \theta - 0.1)}{P_0 + \rho g H - P} \cdot \left(1 + \frac{\delta}{W}\right) \quad [11]$$

Although the environmental pressure P_0 is constant in most cases, the residual pressure P can be adjusted by some pressure control equipment. The influence of these two ambient pressures is also shown in Figure 5. It can be seen from this figure that the residual pressure significantly affects the penetration. Even though it is a little bit larger than the environmental pressure P_0 , liquid metal can be prevented from penetrating the slot plug. To a certain bath depth, the liquid metal bath with

Table I. Physical Properties of Wood's Metal at 101 kPa^[31,32]

Metal	Density (kg/m ³)	Surface Tension (N/m)	Viscosity (Pa s × 10 ⁻³)	Contact Angle θ
Wood's metal [378 K (105 °C)]	9560	0.46	3.26	116.9 deg

Table II. Experimental Conditions used for Dynamical Measurement of the Penetration Behavior

Items	Parameters	Symbol	Value (mm)	
			Group A	Group B
Slot	width	δ	0.12	0.10
	length	W	15	15
Liquid metal bath	depth	H	65	75
Penetration process	maximum depth	h	59.5	19.5

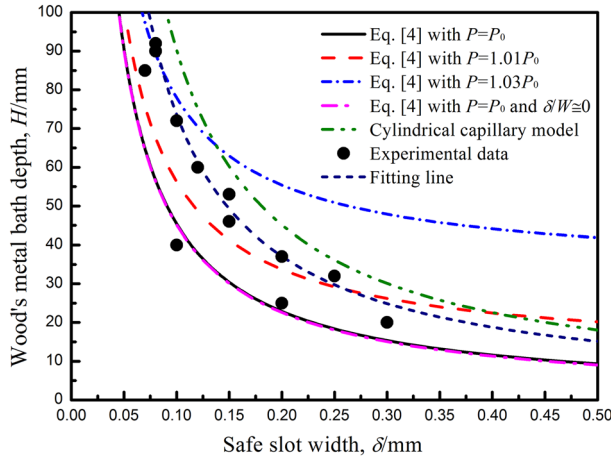


Fig. 5—The relationship between safe slot width and Wood's metal bath depth.

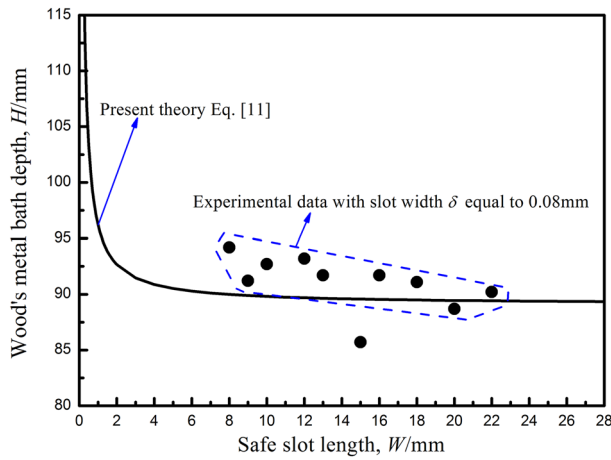


Fig. 6—The relationship between safe slot length and Wood's metal bath depth.

$P > P_0$ can employ a plug with a much wider slot compared with $P = P_0$.

From the curve with $\delta/W \approx 0$ in the figure, it is observed that the influence of slot length on penetration is so little that it can even be ignored. However, it does not mean that such a treatment is applicable and correct in any case. Figure 6 shows the variation of Wood's metal bath depth with a safe slot length; here the slot width δ equals to 0.08 mm. Although there is no experimental data in the range of slot length below 8 mm, the result matches very well with the predicted

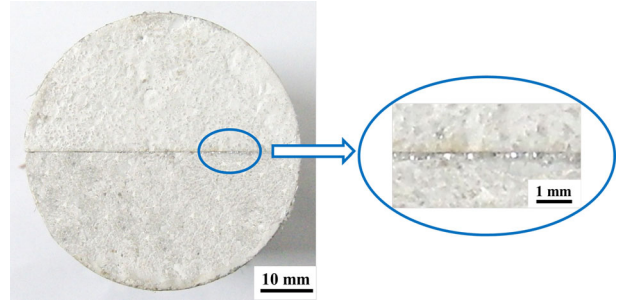


Fig. 7—Top view of the penetration of Wood's metal into a plug with one slot.

curve. When the length is 50 times larger than the width, the bath depth of Wood's metal would not have an obvious change with the variation of slot length. It means that only when the slot width and length sizes are closer, the length has an appreciable influence on penetration. It also confirms that it is reasonable to elide the term of δ/B in Eq. [4] as the length is large enough. Figure 7 shows the top view of the penetration of Wood's metal into a slot plug, where the penetration trace can be observed clearly.

B. An Application of the Prediction Model

As mentioned above, the design and manufacture of a powder injection plug is the key step for developing the new ladle refining process with bottom powder injection, and its resistance ability from penetration is a major factor of concern. Thus, the model is attempted to guide the slot plug design, and Eq. [11], the available form of Eq. [8], is applied to predict the safe slot width.

The variations of ladle bath depth with a safe slot width under different conditions are presented in Figure 8. Obviously, the residual pressure plays a more important role in the region of larger bath depth, and it should be taken into full consideration in the design process. The ideal surface model can not be directly applied to calculate the safe slot width as to its lower prediction, while the classic cylindrical capillary model is also not comprehensive as it ignores too many influential factors. Equation [8], as the basic equation of the current model, can exactly predict the safe slot width; thus, it will be employed to conduct slot parameters.

In general, the depth of ladle bath with a capacity of no more than 60 tons is usually less than 1.5 m,^[33] and the bath depth for the capacity of 150 tons is within 2 to 3 m. In the actual refining process, the correction

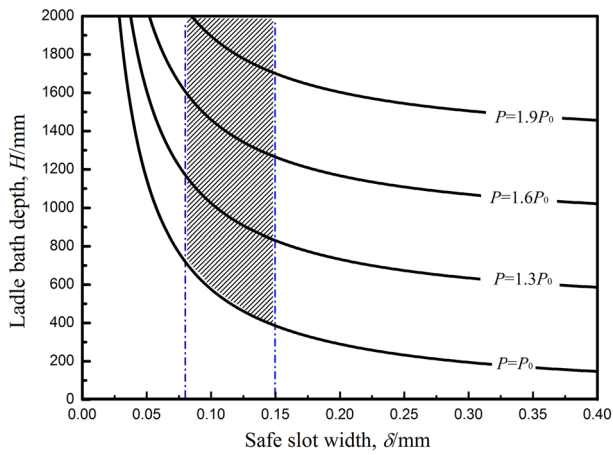


Fig. 8—Variation of the ladle bath depth with safe slot width predicted by Eq. [11].

coefficients k and d are usually larger than those in the current experiment, and the theoretical curve from Eq. [11] will be above the one in Figure 8. Therefore, taking comprehensively all influential factors into consideration, it is reasonable to set the safe slot width in range of 0.08 to 0.15 mm for the bottom powder injection plug as shown in the shaded region in Figure 8. For the slot length, the value is usually 100 times the width.

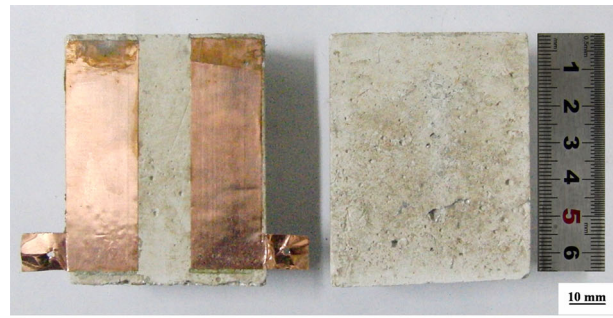
C. Penetration Behavior of Liquid Metal into Slot Plug

1. Dynamic measurement results

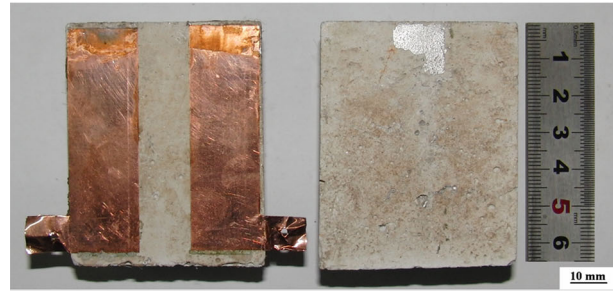
If the slot width is large enough, then penetration of liquid metal into the plug will take place. Then, the penetration behavior needs to be concerned. To describe penetration behavior comparably and exactly, the moment when penetration occurs is specified as the penetration starting point.

The images in Figure 9 show the penetration of Wood's metal into a slot plug at a different time. They were taken from the experiment of Group A. From these images, the penetration process can be directly observed. Combined with the measured profile of the relationship between penetration depth and time in Figure 10(a), the flow behavior of Wood's metal in the slot is clear. It is interesting that the penetration process can be divided into three stages:

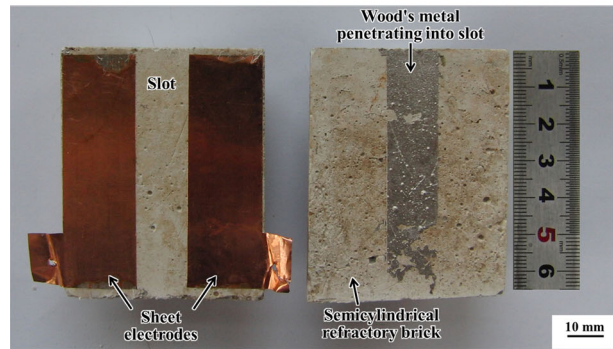
- (a) Stage I: Unsteady penetration stage. At this stage, there are several substages. At some substage, the penetration depth changes sharply with time, whereas at another one, penetration depth may change slowly. Sometimes, the penetration even stops transiently.
- (b) Stage II: Main penetration stage. At this stage, the penetration depth changes sharply with time, and it contributes the largest proportion in the whole penetration depth.
- (c) Stage III: Terminal penetration stage. At this stage, the penetration depth does not change any more, and the value reaches maximum.



(a) $t=0$ s



(b) $t=20$ s



(c) $t=550$ s

Fig. 9—Wood's metal penetrating into the slot of corundum brick at penetration times of (a) 0 s, (b) 4 s, and (c) 550 s.

In detail, Figure 10(a) shows the variation of penetration depth with time in the experiment of Group A. In this group, the Wood's metal bath depth is 65 mm and the slot width is 0.12 mm with a slot length of 15 mm. As can be seen from the figure, stage I of the penetration process lasts for about 90 seconds, and the penetration depth is almost up to 29 mm. During this stage, the penetration depth first grows with penetration time, and then the penetration rate slows down. Obviously, this unsteady stage has not been observed in previous studies on the penetration into porous refractories.^[21–24,27] The following is the main penetration stage, which lasts for about 100 seconds. The penetration depth in this stage increases sharply with penetration time, and finally it reaches the maximum value. Then, penetration gets into stage III, and the penetration depth stays at 59.5 mm.

To verify that the results obtained are not occasional, another set of experiments was carried out subsequently. Similar penetration behavior has also been measured. Figure 10(b) shows the variation of penetration depth

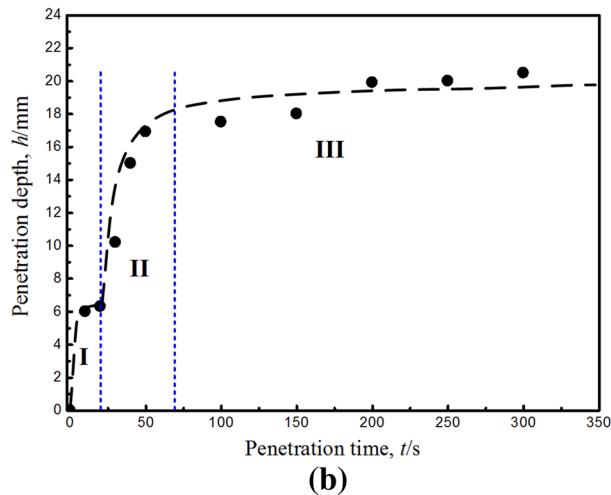
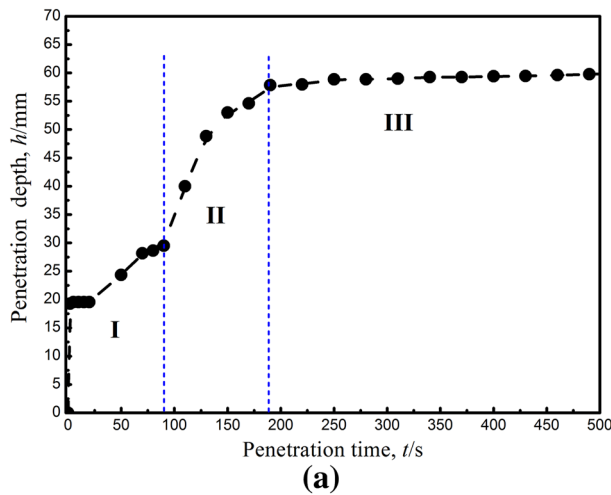


Fig. 10—Experimental results of the variation of the penetration depth with time (a) Group A: slot cross section size 15 mm × 0.12 mm, liquid metal bath depth 65mm, and (b) Group B: slot cross section size 15 mm × 0.10 mm, liquid metal bath depth 75mm.

with time in the experiment of Group B. In this group, the Wood’s metal bath depth is 75 mm, the slot width is 0.10 mm, and the slot length is 15 mm. Obviously, the penetration process can also be divided into three stages. Stage I consists of two substages and lasts about 20 seconds to reach a penetration depth of about 6.3 mm. Then, penetration enters into stage II, and the penetration depth comes to about 18 mm within 40 seconds. After that, penetration reaches stage III, and the penetration depth almost keeps the terminal value of 18 mm.

2. Analysis on the penetration behavior

According to the penetration experiments of molten silver,^[16] mercury, molten steel,^[17] and even slag,^[22] into porous refractory, and of liquid metals into packed ceramic,^[34] Kaptay and his coworkers^[18] proposed a model with periodically changing capillary as illustrated in Figure 11(a). This model is able to describe the variation of maximum penetration depth with external pressure very well, and the penetration diagram has

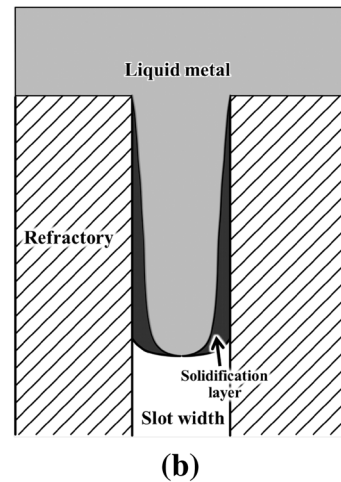
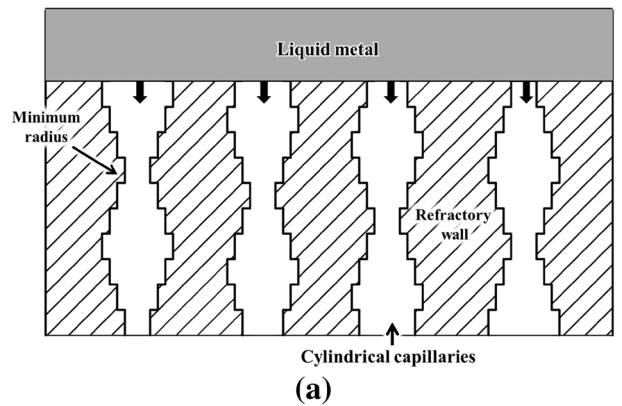


Fig. 11—Schematic illustration of (a) the cylindrical capillary model with periodically changing radii given by Kaptay *et al.*^[18] and (b) the slot penetration model with solidification layer of liquid metal.

been divided into “prepenetration” stage and “bulk-penetration” stage. The governing equations for the penetration rate denoted as the variation of penetration depth with time were derived from Washburn’s model. In this model, at the initial stage, the penetration depth h is linearly dependent as a function of $t^{1/2}$ ^[18] as verified in References 21 and 22, whereas it is quite different from the penetration behavior of liquid metal into the slot plug. The penetration process in a slot plug is divided into three stages, which has never been observed in the previous studies. So if the periodically changing capillary model for porous refractory is unavailable for a slot plug, then an attempt needs to account for the penetration phenomenon of liquid metal into the slot. The details is shown as follows.

As known, the slot length is much larger than the width. In the length direction, there are some potential penetration points where liquid metal spreads on the surface easily due to the inherent inhomogeneity of refractory material. Alternatively, on these points, the width of the slot is a bit larger than other places. Once the penetration points appear, liquid metal will rapidly flow down and go into the slot. While for other parts of the slot, penetration may have not begun or will occur later. In other words, penetration depths along the

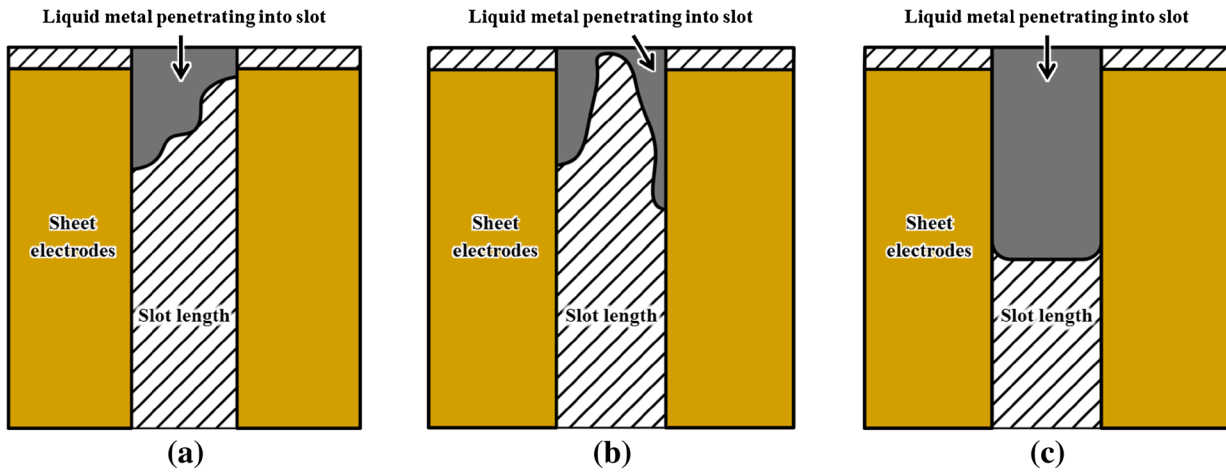


Fig. 12—Schematic illustration of the penetration process of liquid metal into slot: (a and b) at the unsteady penetration stage and (c) at the main penetration stage.

length direction do not keep the same all the time. These are illustrated in Figures 12(a) and (b), and they are observed in the current experiment as shown in Figure 9(b). Because the variation of penetration depth with time was dynamically monitored by the electric signal between the two electrodes, the unsteady penetration stage has been measured.

With the generation of the new penetration points and the growth of old ones, these points or sub-faces would touch with each other and form a face of penetrating liquid metal. When the face would spread out in the whole length direction, penetration comes into the stage II, as illustrated in Figure 12(c).

Due to the cooling effect of the slot wall, when liquid metal spreads into the slot plug, its properties would change gradually. For example, the cooling of the slot wall would increase the viscosity and surface tension, and will decrease the fluidity of liquid metal. Therefore, some liquid metal on the slot wall would form a solidification layer. With the increase of cooling intensity downward, the solidification layer grows thicker and thicker. It implies that the actual slot width is becoming narrow with the increase of penetration depth, which is illustrated with Figure 11(b). Equation [2] shows that the additional pressure, which is the key force to balance with static pressure, increases with the decrease of the slot width and liquid metal surface tension. So, it can be understood that the additional pressure increases with the penetration depth of liquid metal, whereas the penetration velocity decreases gradually. As the penetration comes into the terminal stage, the penetration depth reaches the maximum value. For the porous refractory, the penetration may stop at the minimum diameter of the vertical capillary as shown in Figure 11(a). However, the penetration into the slot plug stops at the bottom of solidification layer where the additional pressure balances with static pressure again.

In the actual process, the nonuniform slot width along the length direction will produce more probabilities of the unsteady penetration, which is extremely harmful to the service reliability of the slot plug. Hence, it is

necessary to strictly control the uniformity of slot width along the length direction.

V. CONCLUSIONS

Penetration phenomenon of liquid metal into slot plug was investigated theoretically and experimentally. A penetration model predicting the relationship of plug parameters and liquid metal bath depth was proposed, and corresponding experimental validation was successfully performed with Wood's metal. Equation [8] was proposed to predict the safe slot width of the plug for bottom powder injection in refining ladles. Based on the new experimental approach by measuring the electrical signal, penetration behaviors have been dynamically monitored. The findings are as follows:

1. The failure of additional pressure against static pressure is the major cause of penetration. The safe slot width preventing penetration is proposed as Eq. [8], in which the influence of slot parameters (including geometric shape and surface roughness), ambient pressures, *etc.*, are all included. Through fitting the results of Wood's metal penetrating into a slot plug, a set of correction coefficients $k = 1.45$ and $d = 0.1$ have been given out.
2. Slot length also affects penetration though not enough to be noticeable. If its value is less 50 times than that of the width, then the effect will become sensible and have to be taken into account.
3. The new experimental approach is very helpful for monitoring penetration. The penetration process of Wood's metal into slot plug is divided into three stages, namely unsteady penetration stage, main penetration stage, and terminal penetration stage. The unsteady stage, caused by nonuniform slot width or inhomogeneous wetting, is made up of several substages, and the main stage contributes to the largest penetration depth, whereas the terminal stage keeps almost a constant penetration depth. It can reduce the chances of unsteady penetration by strictly

controlling the uniformity of slot width along the length direction.

ACKNOWLEDGMENTS

The authors wish to express thanks to the National Natural Science Foundation of China (Grant No. 51134009) and Specialized Research Found for the Doctoral Program of Higher Education (Grant No. 20110042110010)

REFERENCES

1. S.S. Pan, M.Y. Zhu, and J.A. Zhou: *China Metall.*, 2007, vol. 7, pp. 41–43.
2. M.Y. Zhu, J.A. Zhou, S.S. Pan, and J. Sha: Chinese Patent, CN200510047980.1, 2006.
3. M.Y. Zhu, J.A. Zhou, S.S. Pan, and J. Sha: Chinese Patent, CN200520094580.1, 2007.
4. L.R. Farias and G.A. Irons: *Metall. Trans. B*, 1985, vol. 16B, pp. 211–25.
5. D.E. Langberg and M. Nilmani: *Metall. Mater. Trans. B*, 1994, vol. 25B, pp. 653–60.
6. D.E. Langberg, S. Avery, and M. Nilmani: *Metall. Mater. Trans. B*, 1996, vol. 27B, pp. 773–79.
7. M. Numata and Y. Higuchi: *ISIJ Int.*, 2012, vol. 52, pp. 2019–25.
8. I. Sasaka: *Taikabutsu*, 1993, vol. 45, p. 678.
9. S. Niwa, C. Iwasawa, and K. Hayamizu: *Taikabutsu*, 1991, vol. 43, pp. 241–45.
10. T. Matsushita and T. Ohuchi: *Taikabutsu*, 2002, vol. 54, pp. 221–25.
11. Z. Li, K. Mukai, Z. Tao, T. Ouchi, I. Sasaka, S. Iitsuka, and K. Asano: *Taikabutsu*, 1999, vol. 51, p. 594.
12. Z. Li, T. Ouchi, K. Mukai, Z. Tao, I. Sasaka, S. Iitsuka, and K. Asano: *Taikabutsu*, 1999, vol. 51, p. 595.
13. T. Matsushita, K. Mukai, and T. Ouchi: *Taikabutsu*, 2002, vol. 54, p. 128.
14. T. Matsushita, T. Ohuchi, and K. Mukai: *J. Tech. Assoc. Refract. Jpn.*, 2003, vol. 23, pp. 15–19.
15. K. Mukai, Z. Li, Z. Tao, T. Ouchi, I. Sasaka, and S. Iitsuka: *Trans. JWRI*, 2001, vol. 30, pp. 377–82.
16. Z. Li, K. Mukai, Z. Tao, T. Ouchi, I. Sasaka, and S. Iizuka: *Taikabutsu*, 2001, vol. 53, pp. 577–87.
17. T. Matsushita, K. Mukai, T. Ohuchi, I. Sasaka, and J. Yoshitomi: *J. Tech. Assoc. Refract. Jpn.*, 2004, vol. 24, pp. 108–13.
18. G. Kaptay, T. Matsushita, K. Mukai, and T. Ohuchi: *Metall. Mater. Trans. B*, 2004, vol. 35B, pp. 471–86.
19. R.J. Good: *J. Colloid Interface Sci.*, 1972, vol. 42, pp. 473–77.
20. Z. Yu, K. Mukai, K. Kawasaki, and I. Furusato: *J. Ceram. Soc. Jpn.*, 1993, vol. 101, pp. 533–39.
21. K. Mukai, Z. Tao, K. Goto, Z. Li, and T. Takashima: *J. Tech. Assoc. Refract. Jpn.*, 2001, vol. 21, pp. 3–10.
22. K. Mukai, Z. Tao, K. Goto, Z. Li, and T. Takashima: *Scand. J. Metall.*, 2002, vol. 31, pp. 68–78.
23. Z. Kou, T. Fan, and L. Zhang: *Naihuo Cailiao*, 2001, vol. 35, pp. 92–94.
24. H. Barthel and D. Gortan: *Unitec'89. Proc. Unified Int. Tech. Conf. Refractories*, 1989, vol. 1, pp. 555–60.
25. T. Ouchi, A. Mizobe, M. Harada, T. Kaneko, S. Hara, M. Yamamoto, and R. Nishiyama: *Taikabutsu*, 1994, vol. 46, pp. 646–47.
26. D.M. Spori, T. Drobek, S. Zürcher, M. Ochsner, C. Sprecher, A. Mühlebach, and N.D. Spencer: *Langmuir*, 2008, vol. 24, pp. 5411–17.
27. B. He, N.A. Patankar, and J. Lee: *Langmuir*, 2003, vol. 19, pp. 4999–03.
28. N.A. Patankar: *Langmuir*, 2004, vol. 20, pp. 7097–102.
29. W. Li and A. Amirfazli: *Adv. Colloid Interface Sci.*, 2007, vol. 132, pp. 51–68.
30. A. Verma and J.W. Evans: *Metall. Mater. Trans. B*, 1994, vol. 25B, pp. 937–39.
31. M. Iguchi and H. Tokunaga: *Metall. Mater. Trans. B*, 2002, vol. 33B, pp. 695–702.
32. M. Iguchi, T. Nakatani, and H. Tokunaga: *Metall. Mater. Trans. B*, 1997, vol. 28B, pp. 417–23.
33. J. Feng, L. Ai, and J. Liu: *Hot Metal Pretreatment and Molten Steel Secondary Refining*, Metallurgy Industry Press, Beijing, China, 2006, pp. 178–8.
34. C. Garcia-Cordovilla, E. Louis, and J. Narciso: *Acta Mater.*, 1999, vol. 47, pp. 4461–79.